Human engineered meniscus transcriptome after short-term combined hypoxia and dynamic compression

Alexander RA Szojka[1] , Rita de Cássia Marqueti[1,2],
David Xinzheyang Li[1,3] , Clayton W Molter[1], Yan Liang[1],
Melanie Kunze[1], Aillette Mulet-Sierra[1],
Nadr M Jomha[1] and Adetola B Adesida[1]

Abstract

This study investigates the transcriptome response of meniscus fibrochondrocytes (MFCs) to the low oxygen and mechanical loading signals experienced in the knee joint using a model system. We hypothesized that short term exposure to the combined treatment would promote a matrix-forming phenotype supportive of inner meniscus tissue formation. Human MFCs on a collagen scaffold were stimulated to form fibrocartilage over 6 weeks under normoxic (NRX, 20% O_2) conditions with supplemented TGF-β3. Tissues experienced a delayed 24h hypoxia treatment (HYP, 3% O_2) and then 5 min of dynamic compression (DC) between 30 and 40% strain. Delayed HYP induced an anabolic and anti-catabolic expression profile for hyaline cartilage matrix markers, while DC induced an inflammatory matrix remodeling response along with upregulation of both *SOX9* and *COL1A1*. There were 41 genes regulated by both HYP and DC. Overall, the combined treatment supported a unique gene expression profile favouring the hyaline cartilage aspect of inner meniscus matrix and matrix remodeling.

Keywords

Human engineered meniscus, transcriptome, hypoxia, mechanical loading, dynamic compression

Introduction

The menisci are specialized tissues that perform important mechanical roles in the knee joint including weight bearing.[1,2] Their inner regions are avascular and non-healing in adults.[3] Injuries to the inner regions disrupt function and predispose the knee to early osteoarthritis development.[4] Arthroscopic partial meniscectomy is a common treatment for non-healing inner meniscus tears, but it is also associated with early osteoarthritis development.[5] Meniscus tissue engineering aims to generate functional meniscus tissue constructs that can replace damaged and non-healing native meniscus tissue to restore function and delay osteoarthritis development.

The inner meniscus regions are fibrocartilaginous in adults.[6] The extracellular matrix is composed primarily of type I collagen organized into bundles that confer tensile properties.[1,7] It also contains hyaline matrix components such as type II collagen and aggrecan that confer compressive properties.[1,7] Meniscus matrix is synthesized and maintained

[1]Department of Surgery, Divisions of Orthopaedic Surgery and Surgical Research, Faculty of Medicine & Dentistry, University of Alberta, Li Ka Shing Centre for Health Research Innovation, Edmonton, AB, Canada
[2]Graduate Program of Rehabilitation Sciences, University of Brasília (UnB), Brasília, Distrito Federal, Brazil
[3]Department of Civil and Environmental Engineering, Faculty of Engineering, University of Alberta, Edmonton, AB, Canada

Corresponding author:
Adetola B Adesida, Department of Surgery, Divisions of Orthopaedic Surgery and Surgical Research, Faculty of Medicine & Dentistry, University of Alberta, Li Ka Shing Centre for Health Research Innovation, 112 Street and 87 Avenue, Edmonton, AB T6G 2E1, Canada.
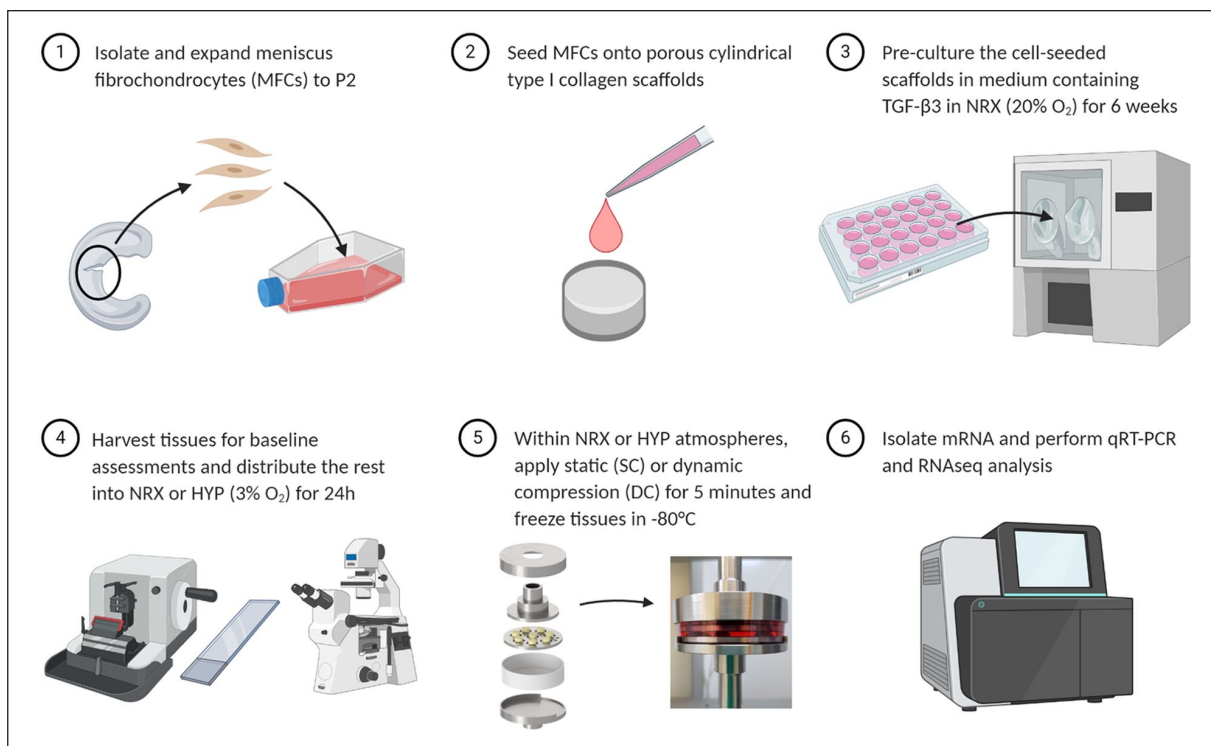Email: adesida@ualberta.ca

Figure 1. Experiment overview. Experiment steps 1–5 were repeated three times, each time using cells from a new human meniscus donor.
Adapted from "Autologous Haematopoietic Stem Cell Transplant", by BioRender.com (2020). Retrieved from https://app.biorender.com/biorender-templates.
HYP: hypoxia; NRX: normoxia; P: passage.

by a heterogeneous population of cells referred to as meniscus fibrochondrocytes (MFCs).[8] MFCs exist natively in a low oxygen and dynamically-loaded environment in adults, experiencing a complex combination of tension, compression, hydrostatic pressure, and shear forces.[1–3,6,9] Low oxygen conditions (known as hypoxia (HYP) or physioxia to reflect the inner meniscus native environment) and mechanical loading such as dynamic compression (DC) can each enhance expression of fibrocartilage matrix components by MFCs in vitro.[10–15] However, little is known about how MFCs respond to these signals simultaneously, and how HYP and mechanical loading can be used in combination toward tissue engineering meniscus.

The objective of this study was to gain a better understanding of how MFCs respond to combined HYP and short-term DC at the global mRNA level using a model system of human meniscus. It was hypothesized that the combined treatment would promote a matrix-forming phenotype supportive of inner meniscus tissue formation.

Materials and methods

Ethics and sample collection

Non-osteoarthritic human meniscus samples from arthroscopic partial meniscectomies as a consequence of trauma at the Grey Nuns Community Hospital and the University of Alberta Hospital in Edmonton were collected with patient consent waived in accordance with the University of Alberta human research ethics board's approval #Pro00018778 to use surgical discards with non-identifying information for scientific research purposes.

Design of a dynamic compression (DC) bioreactor

A custom bioreactor was created out of stainless steel to fit a Biodynamic 5210 test instrument (TA Instruments, USA) positioned inside of a Biospherix X3 incubation chamber system (Supplemental Figure 1). Aspects of the bioreactor design, such as the use of standard Petri dishes to hold samples, were inspired by Mauck et al.[16]

Cell expansion and formation of engineered inner meniscus fibrocartilage

An overview of the experimental methods is provided in Figure 1. Inner meniscus specimens from $n = 3$ independent donors were collected during partial meniscectomy (Figure 2(a)). Meniscus fibrochondrocytes (MFCs) were isolated by collagenase digestion and were expanded to
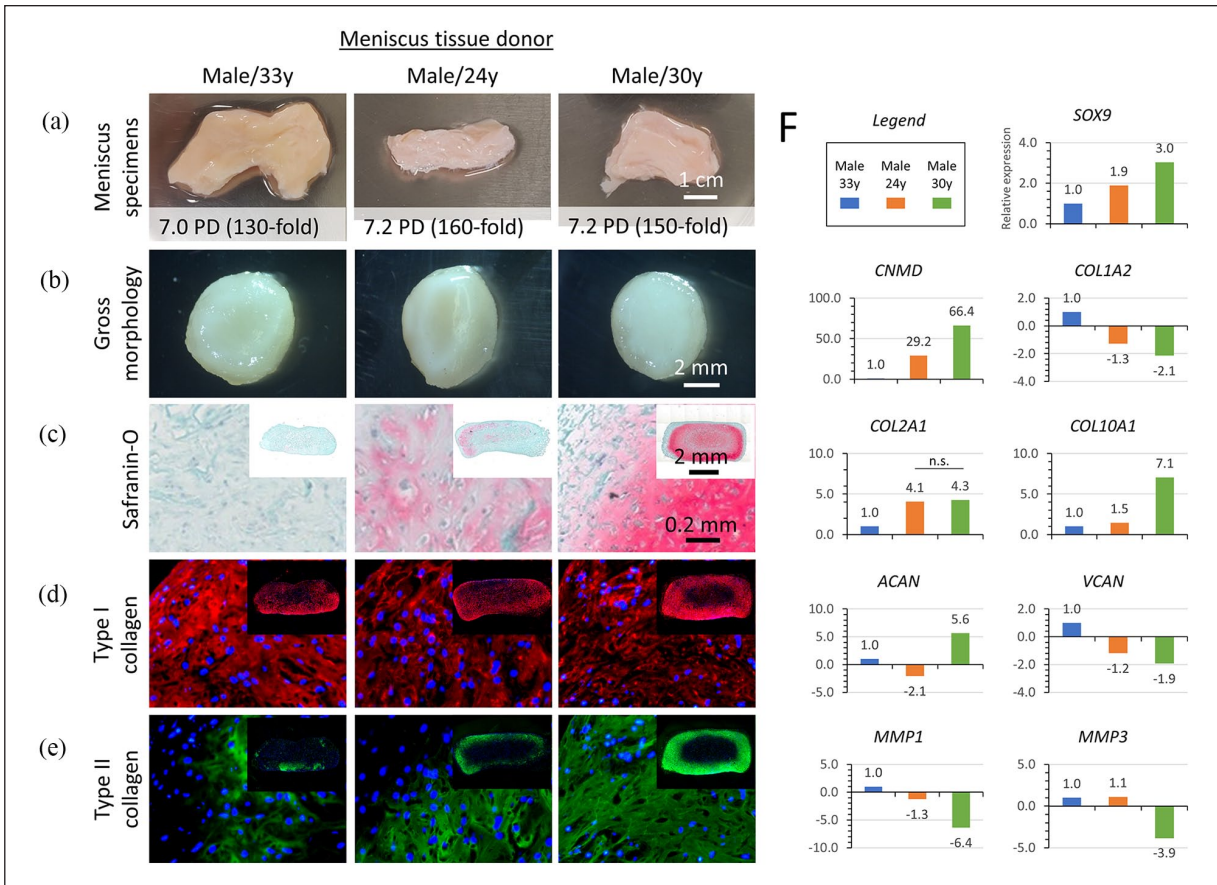
Figure 2. The donors formed a spectrum of engineered meniscus fibrocartilage at the six-week baseline before division into experimental conditions. (a) Gross morphology of the donated meniscus specimens. PD: population doublings reached before scaffold seeding. (b–e) Engineered fibrocartilage gross morphology and staining analysis. Panels in Safranin-O and types I/II collagen rows share common scale bars. Cell nuclei in immunofluorescence images are stained with DAPI (blue). (f) Average expression levels for each donor, pooled across the experimental conditions, for a biased panel of meniscus-related genes. All pairwise comparisons not marked by "n.s." (not significant) were statistically different with $p \leqslant 0.05$.

passage 2 in a high-glucose DMEM containing 1 ng/mL TGF-β1 and 5 ng/mL FGF-2.[17]

MFCs were collected and seeded onto cylindrical type I collagen scaffolds (diameter = 10 mm, height = 3.5 mm, pore size = 115 ± 20 μm, Integra Lifesciences, USA) at a density of 5×10^6/cm^3. The cell-seeded scaffolds were then pre-cultured for 6 weeks in a defined serum-free standard chondrogenic medium containing 10 ng/mL TGF-β3 for fibrocartilaginous matrix formation.[17] The duration was selected based on our unpublished data showing that tissues at this time point contain the primary matrix constituents of the inner meniscus (type I collagen, type II collagen, sulphated proteoglycans) and have substantial mechanical properties compared to shorter culture periods. A study using a similar type I collagen scaffold applied a single dynamic compression event after a comparable preculture period (7 weeks) and found it to have anabolic effects in articular chondrocytes.[18]

At the end of the pre-culture period, baseline tissues were harvested to confirm the presence of fibrocartilaginous matrix using histological staining and immunofluorescence. Briefly, tissues were fixed in formalin and paraffin-embedded, sectioned, and stained with Safranin-O for sulphated proteoglycans and antibodies for types I and II collagens by immunofluorescence.[17]

Experimental conditions (n = 3 donors, 3–4 replicates/condition per donor)

The remaining tissues were randomly assigned into six groups: hypoxia or normoxia with a loading group of either 1. vehicle control (VCtrl), 2. static compression (SC), or 3. dynamic compression (DC). For the oxygen division, tissues were placed into incubation chambers with 3% O_2 (hypoxia, HYP) or 20% O_2 (normoxia, NRX) and 5% CO_2 within an X3 Xvivo system (Biospherix, USA) for a 24 h oxygen tension treatment. This duration was chosen to give time for the medium and tissues to equilibrate to the new environment but not undergo dramatic matrix-level protein changes.

With the atmosphere set to 5% CO_2 with 3% O_2 or 20% O_2, replicate tissues within each group were transferred into Petri dishes containing fresh culture medium and put into the bioreactor. Tissues in a VCtrl group were compressed until reaching a 0.01 N per tissue (Figure 1). The corresponding pre-load position was then re-used for all the five groups so that the strain calculations would be identical. The pre-load position was re-measured for each donor.

VCtrl consisted of samples reaching the pre-load position and then maintained in contact with the platens for 5 min. SC consisted of 30% compression with a five-minute hold. DC consisted of a 30% SC superimposed with 10% cyclic sinusoidal strain at 1 Hz for 5 min. These loading regime strain parameters were selected based upon preliminary work showing that although the tissues underwent rapid stress relaxation during the first minutes of DC loading, the stress response magnitude remained adequate for at least 5 min with these parameters. A study using a similar type I collagen scaffold applied similarly large strains (10% static offset with 25% dynamic amplitude) in articular chondrocytes after a 7 week preculture period and identified the regime to have anabolic effects.[18]

After loading, the samples were removed from contact with the platens and given 30 min to rest for gene expression changes to occur. The samples were then transferred into TRIzol reagent and snap-frozen in liquid nitrogen for storage until the experiment was complete for all three donors.

RNA extraction

Total RNA was extracted with standard chloroform phase separation and isopropanol precipitation.[17] To confirm that the short-term treatments were effective in inducing gene expression changes, RNA was reverse transcribed into cDNA for quantitative real-time polymerase chain reaction (qRT-PCR) with gene-specific primers for loading-sensitive (*c-FOS* and *c-JUN*) and hypoxia-sensitive (lysyl oxidase, *LOX*) genes.[18,19] Chondrogenic regulator *SOX9* was also measured. Gene expression was compared to the average expression levels of three reference genes (Supplemental Figure 2(a), Supplemental Table 1).

SPSS 27 (IBM, USA) was used to compare mRNA expression measured by PCR across the different groups by analysis of variance (ANOVA) with oxygen tension and mechanical loading as fixed effects and donor as a random effect. Mean replicate values within each donor and condition were first calculated. The Shapiro-Wilk test was used to assess normality. The presence of any interactions was first assessed by the significance of the Oxygen tension*Mechanical loading term ($p < 0.05$). In cases of no significant interactions, the significance of the main effects were assessed. In cases where mechanical loading had a significant main effect, pairwise comparisons were made between the levels with no p value corrections applied. Fold changes were later compared between qRT-PCR and RNA-seq using Pearson's correlation (Supplemental Figure 2(c)).

RNA sequencing and bioinformatics

Total RNA samples were purified using RNeasy Mini Kits (Qiagen, Germany) with a DNase digestion step according to the manufacturer's protocol. Equal masses of total RNA from 3 or 4 replicate samples within each condition and within each donor were pooled together to reduce inter-replicate variability (Supplemental Figure 1(b)). To maintain inter-donor biological variation, pooled samples only consisted of replicates from the same donor, that is, samples from different donors were not pooled together. With two oxygen tensions (HYP and NRX), three loading groups (VCtrl, SC, and DC), and three donors, there were thus a total of 18 RNA pools that underwent RNA sequencing.

Next-generation sequencing was performed by the University of British Columbia Biomedical Research Centre. Sequencing was performed on the Illumina NextSeq 500 with 20 million paired end 42 bp × 42 bp reads. Twelve thousand nine hundred and forty-six expressed genes were studied.

RNA sequencing data analysis was performed using Partek® Flow® software, version 9.0.20.0622, Copyright © 2020, Partek Inc., St. Louis, MO, USA. Reads were aligned to the human genome hg38 using STAR-2.7.3a and quantified to a transcript model (hg38-RefSeq Transcript 94; 2020-05-01) using the Partek Expectation/Maximization (E/M) algorithm. Normalization was then conducted on samples with Add: 1.0, TMM and Log 2.0 methods and analysis of variance (ANOVA) was used for differential expression analysis for the oxygen tension, mechanical loading, and donor (random) effects. Differences in gene expression were considered significant if p-values adjusted for the false discovery rate (*q* values) were less than 0.05. For certain comparisons, an absolute fold-change threshold of at least two was also applied. Correlation analysis, principal component analysis (PCA), visualization of differentially expressed genes (DEGs), and Venn diagrams were all conducted in Partek Flow software and further exploratory functional analysis was conducted using Gene Ontology (GO) enrichment.

Results

Baseline data

At the baseline, the donors had formed a spectrum of fibrocartilage tissues with expression comparable for type I collagen (Figure 2(d)) but variable for hyaline cartilage matrix markers (Figure 2(c) and (e)). Average expression levels across experimental conditions between donors of a panel of meniscus-related genes supported these protein-level observations (Figure 2(f)). The more hyaline cartilage-like donors M/24y and M/30y had 29 and 66-fold higher expression of chondromodulin (*CNMD*) compared to the more fibrous M/33y donor. The most highly regulated gene between donors was *CYTL1*, which was 5.5 and 1091-fold
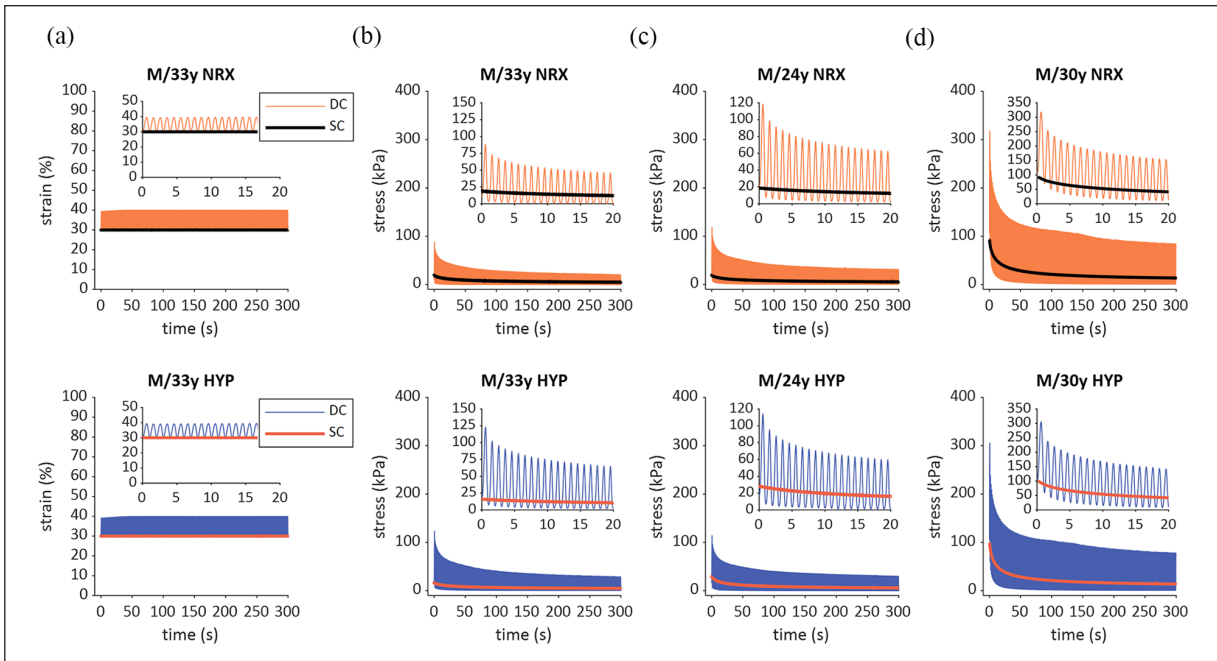
Figure 3. Mechanical loading summary of engineered meniscus fibrocartilage by donor. (a) Strain versus time for a representative donor. (b–d) Average stress versus time, computed as the forces reached during loading divided by the total cross-sectional area of engineered tissues in the bioreactor. The vehicle control groups (no compression) are excluded because the force data is noise. The figure legends in (a) are shared by row.

DC: dynamic compression; HYP: hypoxia, 3% O_2; M: male; NRX: normoxia, 20% O_2; SC: static compression; y: years.

upregulated in M/24y and M/30y respectively compared to M/33y. *BSP1* and *RANKL*, two bone-related genes, showed similar inter-donor trends (*BSP1*: 1, 13.8, and 234-fold; *RANKL*: 1, 4.2, and 86.4-fold).

During loading, the stress versus time plots showed that tissues from the M/30y donor were much stiffer than from the other two donors in both SC and DC groups (Figure 3(b)–(d)). This was consistent with the protein-level histology and IF assessment (Figure 2(c)–(e)).

mRNA level analysis

qRT-PCR analysis. To confirm that the short-term treatments were effective, expression changes in genes sensitive to hypoxia (*LOX* and *SOX9*) and mechanical loading (*c-FOS* and *c-JUN*) were first measured by qRT-PCR. All four genes were significantly upregulated by either HYP or DC, which justified proceeding to more resource intensive RNA sequencing (Supplemental Figure 1(a)).

Principal component (PC) and hierarchical clustering analysis. PCs 1-3 explained 73% of the variance in the RNAseq dataset (Figure 4(a)). There was clustering by oxygen tension and donor factors but not mechanical loading, suggesting that these factors had the largest effects. There were 8475 and 64 genes significantly regulated by oxygen tension and mechanical loading, respectively, indicating that oxygen tension was the more potent treatment than

mechanical loading. It should be appreciated that the treatment durations varied substantially with 24 h for hypoxia and 5 min + 30 min rest for mechanical loading (Figure 4(b)). Hierarchical clustering for oxygen tension separated NRX and HYP samples at the highest level, indicating a robust oxygen tension response across the three donors (Figure 4(c)). Hierarchical clustering analysis for the DC vs. VCtrl samples showed a complete separation between VCtrl and loading groups and a partial separation between SC and DC (Figure 4(d)).

Combined effects of oxygen tension and mechanical loading. There were no genes with statistically significant ($q < 0.05$) two-way interactions between oxygen tension and loading-related treatments, meaning that the effects of loading were not significantly different between oxygen tensions. Of the 8475 and 64 genes respectively regulated by oxygen tension and mechanical loading, 41 were co-regulated by the treatments meaning that they had significant main effects for each (Figure 4(b)). These genes are listed in Table 1. Generally, several of the co-regulated genes are involved in the response to endogenous stimuli and stress such as *ATF3, NR4A3, EGR2, DUSP2/5/6, JUND*, and *KLF4. RGS16* and *SOCS3* play inhibitory roles in signal transduction, while *IER3/5* and *PPP1R15A* play roles in stress resistance and recovery. *ADAMTS1, CCN1* and *PTGS2* are related to matrix remodeling and inflammatory responses, while *CSRNP1/2, MCL1*, and *PHLDA1* are related to apoptosis.
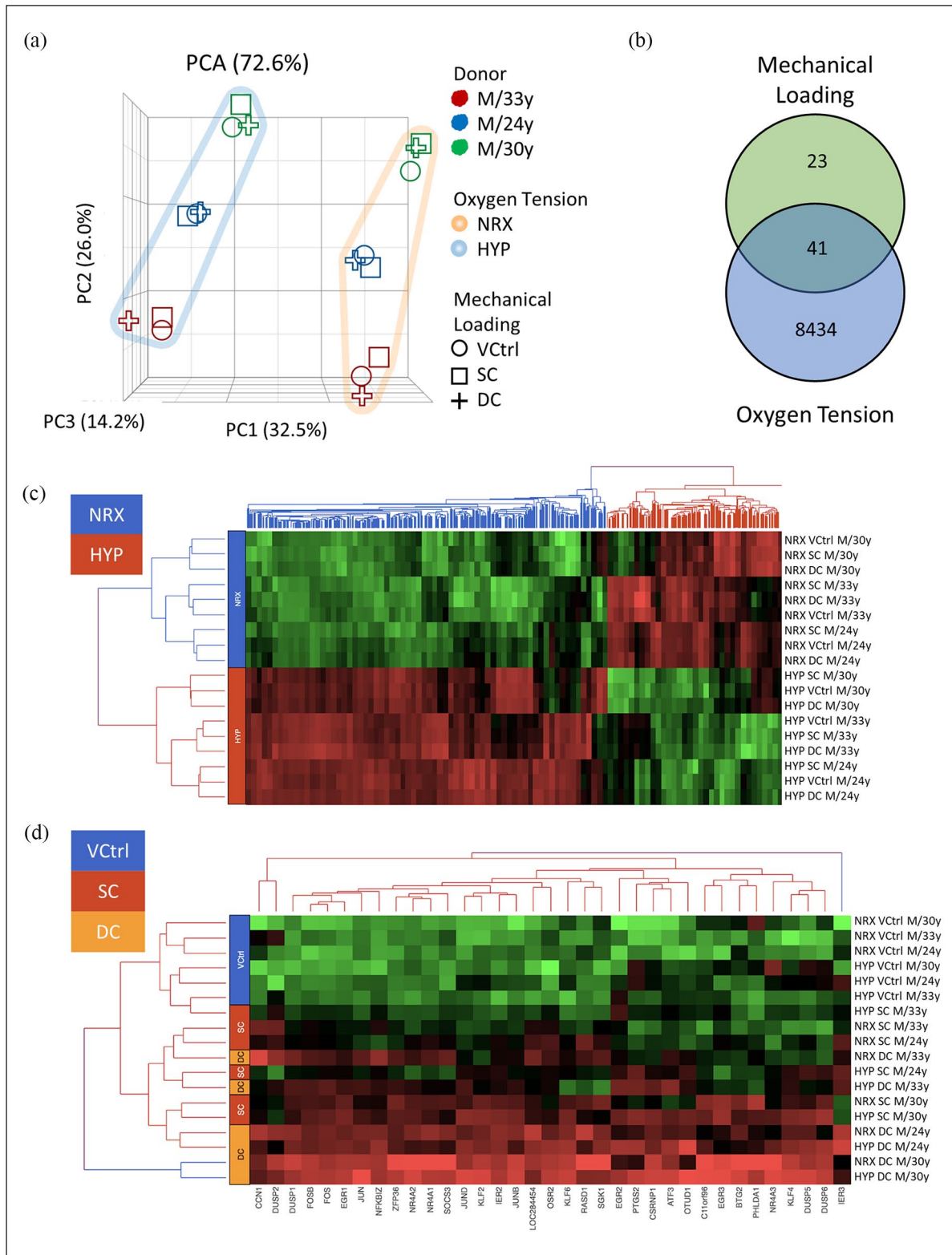
Figure 4. Oxygen tension had a more profound effect than mechanical loading. (a) Principal component analysis. (b) Venn diagram showing genes significantly ($q \leqslant 0.05$) with significant main effects for mechanical loading, oxygen tension, or both. No genes were found with statistically significant two-way interactions between mechanical loading and oxygen tension. (c) Differential expression heatmap and hierarchical clustering analysis of genes regulated at least two-fold between oxygen tensions, narrowing the list of 8475 genes significantly regulated by hypoxia down to 806. The *Z*-score spectrum ranged from −3.12 (green, low expression) to +2.5 (red, high expression). Genes are not labelled for clarity. (d) Similar information as (c) but for mechanical loading. The *Z*-score spectrum ranged from −0.47 to +2.54.

Table 1. Genes significantly co-regulated by oxygen tension and mechanical loading. The HYP versus NRX comparison included nine samples from three donors in each oxygen tension, because the loading groups were combined for this comparison. The SC versus VCtrl and DC versus VCtrl comparisons each contained six samples from three donors because the oxygen groups were combined. Finally, the HYP*DC versus NRX*VCtrl had only three samples from three donors because these were specific groups with no combining possible.

Gene		Fold change			
		HYP versus NRX	SC versus VCtrl	DC versus VCtrl	HYP*DC versus NRX*VCtrl
ADAMTS1	ADAM Metallopeptidase with Thrombospondin Type 1 Motif 1	−2.12*	1.27	1.93*	−1.13
ATF3	Activating Transcription Factor 3	1.87*	2.18*	5.79*	13.38*
CCN1	Cellular Communication Network Factor 1	−1.35*	1.49	2.07*	1.51*
CCNG2	Cyclin G2	2.55*	−1.10	1.04	2.49*
CHD1	Chromodomain Helicase DNA Binding Protein 1	1.12*	1.08	1.28*	1.44*
CHMP1B	Charged Multivesicular Body Protein 1B	−1.31*	1.15	1.50*	1.16*
CLK1	CDC Like Kinase 1	1.88*	−1.10	1.44*	2.62*
CSRNP1	Cysteine and Serine Rich Nuclear Protein 1	1.38*	1.56	2.67*	4.08*
CSRNP2	Cysteineand Serine Rich Nuclear Protein 2	1.13*	1.16	1.34*	1.52*
DUSP2	Dual Specificity Phosphatase 2	−1.61*	1.71	2.90*	1.88*
DUSP5	Dual Specificity Phosphatase 5	1.52*	1.74*	2.81*	5.15*
DUSP6	Dual Specificity Phosphatase 6	1.75*	1.92	3.02*	5.94*
EGR2	Early Growth Response 2	1.56*	1.77*	2.29*	3.99*
GEM	GTP Binding Protein Overexpressed in Skeletal Muscle	−2.72*	1.08	1.59*	−1.72*
HBEGF	Heparin Binding EGF Like Growth Factor	1.45*	1.39	1.71*	2.30*
IER3	Immediate Early Response 3	1.26*	1.49	2.56*	3.70*
IER5	Immediate Early Response 5	1.23*	1.37	1.85*	2.23*
JUND	JunD Proto-Oncogene, AP-1 Transcription Factor Subunit	1.35*	1.78*	2.71*	3.85*
KDM7A	Lysine Demethylase 7A	2.06*	−1.06	1.15	2.29*
KLF4	Kruppel Like Factor 4	1.41*	1.82*	3.20*	4.80*
LOC284454	Uncharacterized LOC284454	−1.28*	2.22*	3.76*	3.21*
MCL1	MCL1 Apoptosis Regulator, BCL2 Family Member	1.12*	1.23	1.64*	1.86*
MIDN	Midnolin	−1.43*	1.35	1.44*	1.01
NR4A3	Nuclear Receptor Subfamily 4 Group A Member 3	1.30*	1.06	2.96*	5.08*
OTUD1	OTU Deubiquitinase 1	1.53*	1.42	2.23*	3.24*
PHLDA1	Pleckstrin Homology Like Domain Family A Member 1	−1.57*	1.52	2.59*	1.65*
PPP1R15A	Protein Phosphatase 1 Regulatory Subunit 15A	2.15*	1.23	1.84*	4.44*
PPP1R3B	Protein Phosphatase 1 Regulatory Subunit 3B	2.23*	−1.31*	−1.19	1.69*
PTGS2	Prostaglandin-Endoperoxide Synthase 2	3.59*	1.86	3.73*	17.11*
RASD1	Ras Related Dexamethasone Induced 1	−2.56*	3.33	9.47*	4.40*
RCAN1	Regulator of Calcineurin 1	2.19*	−1.12	1.21	2.93*
RGS16	Regulator of G Protein Signaling 16	1.85*	1.45	1.90*	3.86*
RND3	Rho Family GTPase 3	−1.15*	1.14	1.57*	1.36*
RSBN1	Round Spermatid Basic Protein 1	1.43*	−1.21*	−1.04	1.31*
SGK1	Serum/Glucocorticoid Regulated Kinase 1	−1.39*	1.54	2.28*	1.67*
SLC25A25	Solute Carrier Family 25 Member 25	−1.41*	1.37	1.51*	1.11
SLC2A3	Solute Carrier Family 2 Member 3	3.29*	−1.17	1.12	3.29*
SOCS3	Suppressor of Cytokine Signaling 3	−1.65*	2.19	5.78*	3.79*
TRIB1	Tribbles Pseudokinase 1	1.69*	1.28	1.78*	3.02*
ZFP36L2	ZFP36 Ring Finger Protein Like 2	−1.59*	1.45	1.62*	1.01
ZNF507	Zinc Finger Protein 507	−1.16*	1.14	1.21*	1.05

*$q \leqslant 0.05$.

Biological interpretation was performed using Gene Ontology (GO) enrichment analysis using the list of co-regulated genes. Selected pathways are presented in Table 2, with the complete pathway listing in Supplemental Table 3. The significantly enriched pathways included several relating to basic cellular functions such as catalytic activity and metabolic processes, as well as cellular signalling such as MAP kinase.

Table 2. Selected enriched pathways from Gene Ontology (GO) analysis of genes co-regulated by oxygen tension and mechanical loading, as well as the individual effects of each treatment. The full lists are available in Supplemental Tables 3 to 5.

Description	*p*-value	Genes in list
GO Pathway: 41 oxygen and mechanical loading regulated genes (FDR ≤ 0.05)		
Regulation of smooth muscle cell proliferation	5.88E–7	6
Regulation of phosphate metabolic process	8.79E–7	16
MAP kinase tyrosine/serine/threonine phosphatase activity	3.82E–6	3
Regulation of catalytic activity	6.3E–6	17
Regulation of cellular metabolic process	1.01E–5	28
GO Pathway: 806 hypoxia versus normoxia genes (FDR ≤ 0.05, |FC| ≥ 2)		
Endoplasmic reticulum unfolded protein response	4.98E–15	29
Signal transduction	9.55E–15	262
Response to endoplasmic reticulum stress	2.89E–14	44
Extracellular space	8.81E–14	105
Response to hypoxia	2.16E–12	41
Angiogenesis	1.27E–10	39
Extracellular matrix	2.17E–10	54
Ion homeostasis	2.44E–10	66
Collagen-containing extracellular matrix	5.77E–8	41
GO Pathway: 35 DC versus VCtrl genes (FDR ≤ 0.05, |FC| ≥ 2)		
Response to endogenous stimulus	3.3E–14	18
Positive regulation of RNA metabolic process	1.02E–13	21
DNA-binding transcription factor activity	2.53E–13	18
Positive regulation of cellular metabolic processes	3.98E–12	25
Response to hormone	5.43E–12	14
Positive regulation of cellular biosynthetic process	1.95E–11	20
Transcription factor AP-1 complex	1.96E–11	4
Cell differentiation	2.7E–11	19

Table 3. Genes with the largest |FC| between HYP and NRX.

Oxygen regulated DEGs with the 10 largest fold changes

Genes		Fold change		
		HYP versus NRX	SC versus VCtrl	DC versus VCtrl
BHLHA15	Basic Helix-Loop-Helix Family Member A15	30.94*	1.08	1.02
KISS1R	KISS1 Receptor	30.52*	−1.12	−1.00
KTI12	KTI12 Chromatin Associated Homolog	−26.75*	1.07	−1.52
CDH15	Cadherin 15	18.43*	−1.26	1.03
ARFGEF3	ARFGEF Family Member 3	18.23*	1.11	−1.03
P2RY11	Purinergic Receptor P2Y11	16.59*	2.72	4.21
MT3	Metallothionein 3	14.88*	1.01	1.10
DERL3	Derlin 3	14.78*	1.18	1.33
STC1	Stanniocalcin 1	14.69*	1.12	−1.11
CKMT2	Creatine Kinase, Mitochondrial 2	13.55*	1.23	1.09

*q ≤ 0.05.

Characterization of individual main effects for oxygen tension and mechanical loading. Of the 8475 genes regulated by oxygen tension, 806 had absolute value fold-changes, |FC| ≥ 2. The ten genes with the highest fold changes are shown in Table 3, with the complete list available in Supplemental Table 2. The 24h hypoxia treatment had profibrocartilage effects including upregulation of anabolic genes including *SOX9* (1.58-fold), *FGF-1* (3.29-fold),

MATN4 (2.39-fold), and *ACAN* (1.49-fold), and downregulation of catabolic genes *ADAMTS1* (2.12-fold) and *MMPs 1, 3, and 13* (4.50, 2.98, and 1.59-fold respectively). Selected enriched pathways from GO analysis are presented in Table 2, with the complete listing available in Supplemental Table 4.

Of the 64 genes regulated by mechanical loading, 35 genes had |FC| ≥ 2. All of these fell within the DC versus VCtrl

Gene	VCtrl	SC	DC
(DC vs. VCtrl) only			
RASD1	1	3.3	9.5*
SOCS3	1	2.2	5.8*
ERG3	1	2.8	4.4*
C11orf96	1	1.9	4.1*
KLF2	1	2.4	4.0*
JUN	1	1.7	3.3*
OSR2	1	2.0*	3.2*
KLF4	1	1.8*	3.2*
JUNB	1	1.9	3.0*
DUSP6	1	1.9	3.0*
NR4A3	1	1.1	3.0*
DUSP2	1	1.7	2.9*
DUSP5	1	1.7*	2.8*
JUND	1	1.8*	2.7*
CSRNP1	1	1.6	2.7*
NFKBIZ	1	1.7*	2.6*
PHLDA1	1	1.5	2.6*
IER3	1	1.5	2.6*
BTG2	1	1.4	2.4*
ERG2	1	1.8*	2.3*
SGK1	1	1.5	2.3*
OTUD1	1	1.4	2.2*
CCN1	1	1.5	2.1*
KLF6	1	1.5	2.1*

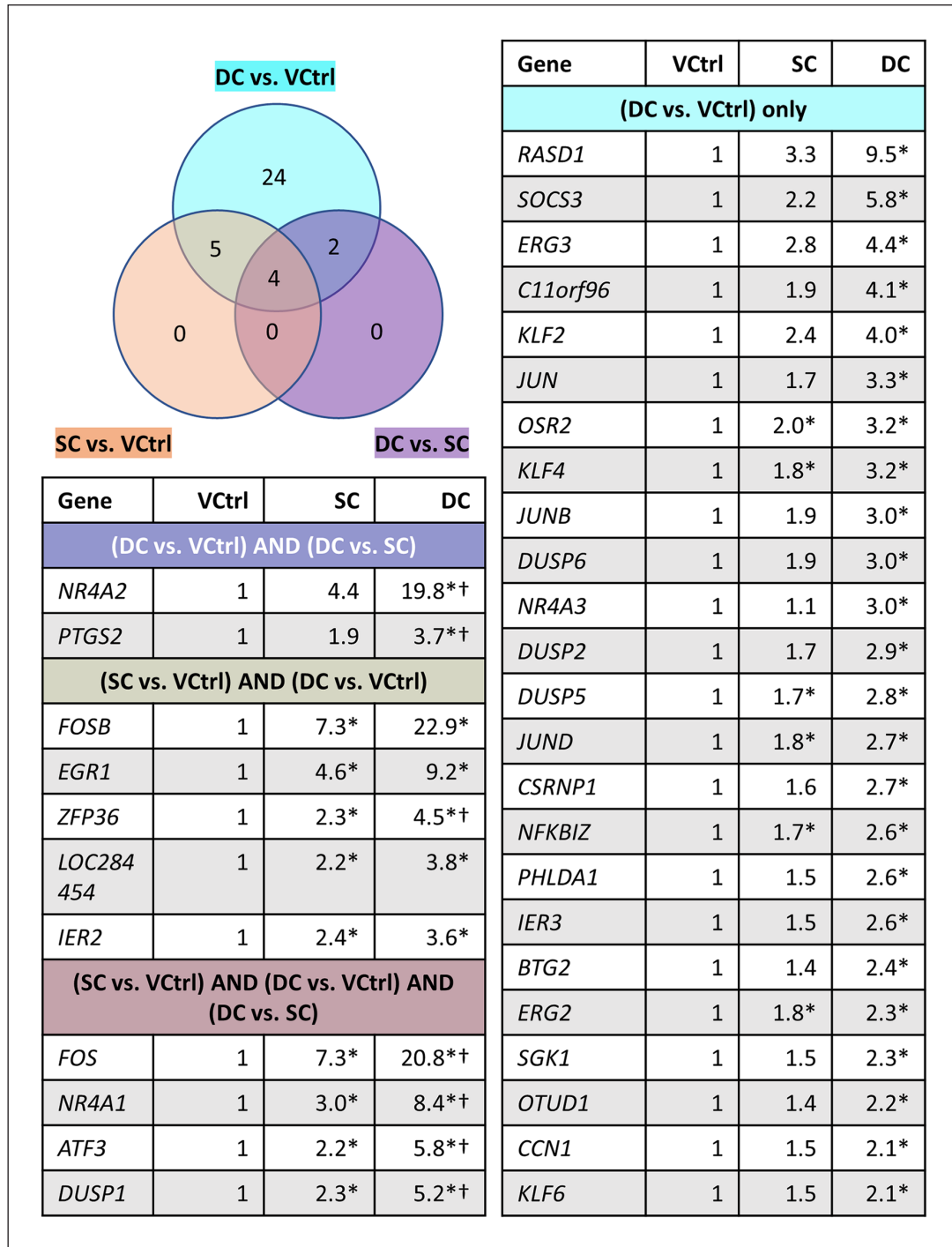| Gene	VCtrl	SC	DC
(DC vs. VCtrl) AND (DC vs. SC)			
NR4A2	1	4.4	19.8*†
PTGS2	1	1.9	3.7*†
(SC vs. VCtrl) AND (DC vs. VCtrl)			
FOSB	1	7.3*	22.9*
EGR1	1	4.6*	9.2*
ZFP36	1	2.3*	4.5*†
LOC284454	1	2.2*	3.8*
IER2	1	2.4*	3.6*
(SC vs. VCtrl) AND (DC vs. VCtrl) AND (DC vs. SC)			
FOS	1	7.3*	20.8*†
NR4A1	1	3.0*	8.4*†
ATF3	1	2.2*	5.8*†
DUSP1	1	2.3*	5.2*†

Figure 5. Dynamic compression was more effective in inducing a gene expression response than static compression. The data is pooled from both oxygen tensions. All listed genes were significantly regulated in at least one of the comparison groups with $q \leqslant 0.05$ and $|FC| \geqslant 2$.
*Significance relative to VCtrl.
†Significance relative to SC.

comparison (Figure 5). These genes all showed a "step-up" in fold change and increased statistical significance in comparing first VCtrl to SC and then SC to DC (Figure 5). This indicates that SC did not upregulate a unique set of genes compared to DC; rather, it induced an intermediate gene expression phenotype between VCtrl and DC. The DC treatment was clearly more effective than the SC treatment in inducing a gene expression response. This is likely due to the dynamic loading aspect but also the added compression applied in DC (up to 40% total strain) compared to SC (up to 30%).

The ten genes with the highest fold-changes in DC versus VCtrl are shown in Table 4, with the complete list

Table 4. Top 10 mechanical loading genes with the highest fold change in DC versus VCtrl.

Gene		Fold change		
		HYP versus NRX	SC versus VCtrl	DC versus VCtrl
Mechanical loading regulated DEGs with the 10 largest fold changes				
FOSB	FosB Proto-Oncogene, AP-1 Transcription Factor Subunit	−1.03	7.26*	22.85*
FOS	Fos Proto-Oncogene, AP-1 Transcription Factor Subunit	1.15	7.30*	20.81*
NR4A2	Nuclear Receptor Subfamily 4 Group A Member 2	−1.37	4.35	19.80*
EGR1	Early Growth Response 1	1.15	4.56*	9.17*
NR4A1	Nuclear Receptor Subfamily 4 Group A Member 1	−1.54	2.95*	8.41*
DUSP1	Dual Specificity Phosphatase 1	−1.18	2.34*	5.21*
ZFP36	ZFP36 Ring Finger Protein	−1.16	2.33*	4.50*
EGR3	Early Growth Response 3	1.05	2.77	4.43*
C11orf96	Chromosome 11 Open Reading Frame 96	1.04	1.19	4.11*
KLF2	Kruppel Like Factor 2	1.24	2.35	3.95*

*$q \leqslant 0.05$.

Table 5. Expression comparisons between HYP/NRX, DC/VCtrl, and the double versus no treatment groups HYP*DC/NRX*VCtrl for a biased selection of meniscus-related genes. The HYP versus NRX comparison included nine samples from three donors in each oxygen tension, because the loading groups were combined for this comparison. The DC versus VCtrl comparisons each contained six samples from three donors because the oxygen groups were combined. The HYP*DC versus NRX*VCtrl had only three samples from three donors because these were specific groups with no combining possible.

Gene		Fold change		
		HYP versus NRX	DC versus VCtrl	HYP*DC versus NRX*VCtrl
ACAN	Aggrecan	1.49*	1.08	1.56*
ADAMTS1	ADAM Metallopeptidase with Thrombospondin Type 1 Motif 1	−2.12***	1.93***	−1.13
COL1A1	Collagen Type I Alpha 1 Chain	−1.19	1.33*	1.16
COL2A1	Collagen Type II Alpha 1 Chain	1.20	1.16	1.31
COL10A1	Collagen Type X Alpha 1 Chain	1.23	1.04	1.16
DCN	Decorin	−1.21***	1.00	−1.23***
MMP1	Matrix Metallopeptidase 1	−4.50***	1.07	−4.68***
MMP3	Matrix Metallopeptidase 3	−2.98***	1.03	−2.80***
MMP13	Matrix Metallopeptidase 13	−1.59***	1.08	−1.5*
SOX9	SRY-Box Transcription Factor 9	1.58***	1.37*	2.09***
VCAN	Versican	−2.04***	1.03	−1.96***

*$p < 0.05$. ***$p < 0.001$.

provided in Supplemental Table 2. Several genes related to the AP-1 transcription factor complex, including *FOS, FOSB, JUN,* and *JUNB* were upregulated with roles in early signal transduction of mechanical stimulus. Further, many genes involved in inflammatory-related pathways such as MAPK, IL-17, and TNF signalling were also upregulated. Selected enriched pathways from GO analysis of the 35 genes significantly regulated by mechanical loading with |FC| ⩾ 2 are presented in Table 2, with the complete listing available in Supplemental Table 5.

A biased panel of known meniscus fibrocartilage matrix-related genes were then considered to assess whether the combined treatment had beneficial effects for tissue formation at this early stage using unadjusted *p* values (Table 5). HYP clearly favoured matrix protection through consistent suppression of catabolic enzymes such as *ADAMTS1* (-2.12-fold) and *MMPs*. It also favoured development of the hyaline cartilage aspects of the inner meniscus through upregulation of *ACAN* (1.49-fold) and *SOX9* (1.58-fold) and suppressed the fibrous aspect through reduced expression of *VCAN* (-2.04-fold), *DCN* (-1.21-fold) (Table 5). DC had mixed effects, increasing both hyaline cartilage-like tissue marker *SOX9* (1.37-fold) and fibrous tissue marker *COL1A1* (1.33-fold), as well as the aggrecanases such as *ADAMTS1* (1.93-fold) (Table 5).

Discussion

This study investigated the global gene expression response of human MFCs to a short mechanical loading event under

different oxygen tensions. Engineered tissues from the three donors were remarkably different in the degree of hyaline cartilage matrix formation at the baseline. Inter-donor variability was also a considerable factor after application of the experimental conditions based upon PCA. The donors appeared evenly spaced from one another on the PCA plot and covered a range of fibrous to cartilaginous matrix phenotype, which may improve the external validity of this study's findings with respect to the oxygen tension and mechanical loading treatments because the listed genes were identified as being significantly regulated across the three donors with differing matrix phenotypes. The RNA pooling strategy from multiple replicates within conditions and donors would have reduced the contributions of variability in culture and analysis, making it easier to detect these differences between donors. Pooled across the experimental conditions, several genes were identified with wide differences in expression levels between donors that correlated to the matrix phenotype, which may prove useful as candidate biomarkers for hyaline cartilage type matrix formation in this model. Previous work has also reported human MFCs to show considerable inter-donor variability.[20] This result highlights the importance of biological replication using multiple meniscus tissue donors.[21]

During the early phases of monolayer expansion, MFCs lose their native expression of chondrogenic markers but these can be restored through 3D culture with TGF-β3.[10,17] However, clearly there were wide inter-donor variations in the degree that MFCs re-express chondrogenic markers. For donors with more chondrogenic MFCs, shorter exposure to pro-chondrogenic conditions may be more appropriate to attain matrix compositions more representative of healthy adult meniscus.[22] The observed inter-donor differences cannot be attributed with certainty to a specific cause. The donors were of the same sex, of similar age, and their cells underwent similar degrees of in vitro expansion.[10,17] Two potential contributors were the proportion of inner vs. outer meniscus tissue in the donor samples and the injury details: the M/33y tissue specimen was more than twice as large as the others implying inclusion of parts of the outer fibrous regions and the M/30y donor had an associated ACL injury. Different injuries could affect the progenitor cell proportion within the harvested meniscus specimen with downstream effects on the matrix-forming capacity of isolated cells.[23–27] Although MFCs may be the most attractive cell type for meniscus tissue engineering applications,[28] it is a challenge that their matrix-forming outcomes may depend upon uncontrollable factors such as the nature of the injury and the recruitment of local stem cell progenitors.[29–32] Candidate gene biomarkers of the human inner avascular meniscus have been characterized relative to expanded and re-differentiated MFCs.[33] Chondroadherin (*CHAD*), which encodes a cartilage matrix adhesion-related protein, showed wide expression differences within that study and in the present work

between the fibrous and hyaline-like donors (11-fold upregulation) with M/24y as the intermediate, suggesting its expression in tissue may provide early knowledge of a donor's downstream matrix forming capacity. Similar methods to predict the matrix-forming capacity of a donor's cells at an early stage may facilitate eventual clinical translation of meniscus tissue engineering-related technology.

The finding of no significant interactions between hypoxia and mechanical loading indicates that gene regulation by a single loading event did not seem to depend on whether the tissues were in a hypoxic or normoxic state at the measured time point. It should be appreciated that the study had limited power to detect statistical interactions. It was, however, interesting to find a list of genes regulated by both oxygen tension and mechanical loading. This indicates that the treatments can amplify or antagonize each other's effects through regulation of the same genes. The rightmost column of Table 1 shows how large combined fold changes could be produced in the double treatment group (HYP/DC) compared to the double control (NRX/VCtrl), as the main effects are multiplied through cooperative co-regulation. For example, *ATF3* (1.9-fold HYP/NRX, 5.8-fold DC/VCtrl) and *PTGS2* (3.6-fold HYP/NRX, 3.7-fold DC/VCtrl) were respectively upregulated 13.4 and 17.1-fold in the double treatment compared to the control. Other genes had antagonistic co-regulation, with the HYP and DC effects neutralizing each other. For example, *ADAMTS1* was suppressed 2.1-fold by hypoxia and induced 1.9-fold by DC. Apart from cooperative or antagonistic co-regulation of specific genes between the oxygen and mechanical loading treatments, the unique genes regulated by the individual treatments are all regulated together in the combined treatment. Simultaneous treatments of oxygen tension and mechanical loading thus induce a unique combined gene expression profile. These genes were identified despite the wide differences in the degree of hyaline cartilage-like matrix between the three donors, suggesting that their expression may be robust to variations in this variable.

Table 5 shows the individual and combined effects of HYP and DC on a list of inner meniscus matrix-related genes. The clearest result was that the combined treatment supported development of a more hyaline cartilage-like matrix profile. The results were otherwise mixed: HYP strongly suppressed catabolic enzymes which was only partly balanced by increases in these enzymes by DC. The HYP and DC treatments also had opposing effects on fibrous tissue markers. This makes sense in the context of the native meniscus because the adult tissue contains both hyaline cartilage and fibrous tissue characteristics. The results thus offer early support for our hypothesis that combined hypoxia and mechanical loading would induce a matrix-forming phenotype favourable to inner meniscus tissue formation. Beyond the inner meniscus, this could be

an important result for the field of hyaline cartilage tissue engineering. However, it remains to be determined how longer treatment durations would affect this profile and to what extent it would translate into protein and mechanical effects.

Previous work in combined hypoxia and mechanical loading in the context of other tissue engineering applications besides meniscus showed similar hypoxia-induced upregulation of hyaline cartilage matrix components as was observed here.[34–36] Hypoxia regulation of HIF-1 is well known to have pro-chondrogenic effects, and was recently shown to mediate anti-catabolic effects through suppression of MMPs as was observed here and by suppression of NF-κB signalling.[37] Previously, HYP increased *SOX9* in MFC cell pellets[38] but did not affect *SOX9* in MFC-seeded type I collagen scaffolds when applied immediately after cell seeding.[39] The results indicate that a delayed hypoxia treatment occurring after a NRX pre-culture period may allow HYP to exert chondrogenic effects in the type I collagen scaffold. This is further supported by yet unpublished data in this same culture model, which showed nearly 5-fold upregulation of *SOX9* for $n=3$ donors after 5 days of culture in HYP compared to NRX following a 3-week NRX pre-culture period.

Static compression (SC) was used as a control group for dynamic compression (DC). Under normoxic conditions, SC under normoxic conditions has been shown to inhibit matrix synthesis and promote matrix breakdown in meniscus and cartilage tissue such as through decreased synthesis of collagen and sulphated proteoglycans, reduced mRNA expression of precursors to type I collagen and proteoglycans such as aggrecan and decorin, and increased mRNA expression of MMP-1.[40–42] In contrast, under normoxic conditions in engineered meniscus and cartilage, DC can have anabolic or catabolic effects depending on the conditions measured through changes in outcomes such as GAG and collagen contents, mechanical properties, matrix organization, and mRNA expression of related genes.[15,18,43–46] Here, the SC treatment had a fundamentally similar response to the DC treatment but with smaller effect sizes and less differential gene regulation. The reason that gene expression in SC was fundamentally like that of DC, that is, pro-fibrocartilage, here may be due to the short treatment duration. Also, since the total level of strain in DC was up to 40% and only 30% in SC, the differences between these groups can't be solely attributed to the dynamic aspect of DC as it could have been due to the added compression. However, the large increase in *c-FOS* in DC (35.8-fold) compared to SC (10.1-fold) relative to the unloaded VCtrl group suggests that the dynamic aspect accounts for much of the difference (Supplemental Figure 2(a)).

Dynamic mechanical loading regimes of cartilaginous tissues such as meniscus may be described on a "loading aggression spectrum" from insufficient (no effects) to excessive (detrimental effects), with an intermediate optimum (beneficial effects).[21,46,47] Placement of a DC regime on the spectrum depends on loading parameters (e.g. applied strains) and the matrix maturity prior to initiation of loading.[21,48] Although the same loading regime applied to native meniscus tissue or in brittle hydrogels would likely be destructive, in our experiences engineered tissues on the porous type I collagen scaffolds can undergo large strains—well beyond 40%—without a dramatic loss of cell viability. The scaffolds themselves are readily compressible, and so the only relevant limits to the strains that can be applied are what the cell-made matrix can withstand. Despite the inter-donor variability in matrix maturity, a common set of genes was rapidly regulated by the short-term mechanical loading indicating a donor independent mechanotransduction response. Many of the genes upregulated by mechanical loading were stress and inflammation related. This suggests that for the maturity of engineered meniscus fibrocartilage used here, the applied loading regime may have been excessive. However, the panel of specific fibrocartilage related genes assessed by unadjusted p-values showed mixed anabolic and catabolic characteristics, with upregulation of a type I collagen precursor and chondrogenic regulator *SOX9*, but also precursors for aggrecanases. This indicates that the load regime induced matrix remodeling activities, which is remarkable given its short duration. The DC-induced increase in *SOX9* observed here is consistent with previous work in chondrocytes in a similar type I collagen scaffold with a single loading event.[18] The few published mechanical loading studies that investigated meniscus engineered with human MFCs all used normoxia and show mixed results, but generally induced anabolic effects such as increased expression of types I and II collagens, *ACAN*, and *SOX9*.[49–53] The initial gene expression profile under DC observed here has promising early effects consistent with previous work and seems especially promising when combined with the matrix protecting and hyaline cartilage promoting effects of HYP.

Peak stress can be used as an indicator for the aggressiveness of a DC regime that cycles between two strain levels. In a similar culture model to the present study but on the last day of two weeks of loading after an initial two-week pre-culture duration, the peak stress during DC from 0 to 10% strain ranged from 1.9 to 2.4 kPa (Szojka, unpublished data). In contrast, the present study's DC groups reached peak stresses from 30 to 40% strain of 88–305 kPa. The pre-culture duration and loading regime in the current study were designed to provide much more aggressive DC loading than the previous work because no mechanotransduction effect had been observed. The beneficial effects of increased static pre-culture time on instantaneous compression modulus from 0 to 10% strain were clear between studies: 4 weeks previously led to a range between donors of 26–40 kPa, whereas 6 weeks here had a range of 57–163 kPa (data not shown). Based on stress values and the

inflammatory gene profile induced here, the two matrix maturity and loading regime combinations are on opposite ends of the loading aggression spectrum. Our ongoing work investigates an intermediate combination of pre-culture duration and loading regime applied over a longer period under HYP and NRX conditions.

Early in life, the human menisci are vascularized and fibrous.[6] By adulthood, the inner meniscus regions transition to an avascular fibrocartilage phenotype with an organized functional matrix of type I collagen and hyaline matrix components.[3,6,54] Development of the adult inner meniscus phenotype is speculated to be related to increased mechanical loading during the first two decades of life, with the strain fields induced by deformational loading potentially guiding organization of the type I collagen.[3,6,54–58] Being avascular and existing within the hypoxic synovial fluid, MFCs within the inner meniscus regions experience a low oxygen tension environment that may assist in development of hyaline cartilage matrix components.[3,9,38] The present study mimicked the low oxygen environment using HYP incubators, and mechanical loading by DC. The results suggest that HYP regardless of loading supports accumulation of hyaline cartilage aspect of fibrocartilage by promoting anabolism and suppressing catabolism. On the other hand, DC regardless of oxygen tension induces a mixed profile suggestive of matrix remodeling. This could be important to protect the integrity of the avascular matrix from loading-induced inflammation.[59,60] The anabolic effects of hypoxia combined with the matrix remodeling effects of an optimized DC regime could help generate engineered meniscus with more physiological characteristics.

This study had two main limitations. The gene expression profiles were considered only at a single time point after loading. Previously, *FOSB* and *SOX9* expression immediately increased after an anabolic loading period and returned to baseline levels within hours in chondrocytes. Although the single time point of 30 minutes may have appropriately captured the early gene expression response to loading, it missed out on delayed and downstream mRNA changes.[18] The study also only considered a single and short-term loading event, and thus the mRNA and protein effects of longer loading durations under HYP compared to NRX remain unknown. Obviously, recurring loading events are more representative of meniscus physiology, and it is likely that longer term treatments would have favoured discovery of interactions between the treatments in individual genes. No protein analysis was performed to validate differences in mRNA content between groups because the harvest time point was so early after the loading period and it was expected that related protein changes would be limited compared to those at the mRNA level. It can thus only be assumed that changes in mRNA expression led to differential protein transcription. The RNAseq data pooled across groups was well supported by baseline protein and mechanical observations, however, making this a plausible assumption (Figures 2 and 3). The stress vs. strain curves during loading showed an initial stress relaxation period followed by a plateau (Figure 3). Our future work will also investigate the effects of DC regimes that extend well into the plateau region, as are typical in related literature.[21]

Conclusion

A short-delayed hypoxia (HYP) treatment after 6 weeks of normoxic pre-culture was enough to induce an inner meniscus matrix-forming phenotype in engineered human meniscus tissue constructs. Early molecular level changes occur in response to static compression that are amplified by dynamic compression (DC). Delayed HYP regardless of loading supports accumulation of hyaline cartilage-type matrix by promoting anabolism and suppressing catabolism. On the other hand, DC regardless of oxygen tensions induces a mixed profile suggestive of matrix remodeling. Several genes were identified that are co-regulated by oxygen tension and compression loading. Altogether, these results indicate that simultaneous HYP and DC are promising as a combined treatment for inner meniscus tissue engineering.

Authorship

All listed authors meet the *Journal of Tissue Engineering* criteria for authorship. AS and ABA designed the study. AS and CM designed the bioreactor. AS and RM performed tissue culture. DL, AS, RM, and MK performed qPCR expression analysis. DL was responsible for RNA-Seq data analysis with Partek Flow software. AS and DL performed statistical analysis and prepared tables and figures. AS and DL wrote the manuscript with input from all co-authors. NMJ assisted with procuring clinical specimens and in reviewing and editing the manuscript. ABA supervised and was responsible for acquiring financial support for the study.

Declaration of conflicting interests

The author(s) declared no potential conflicts of interest with respect to the research, authorship, and/or publication of this article.

ORCID iDs

Alexander RA Szojka [iD] https://orcid.org/0000-0003-0334-9040

David Xinzheyang Li [iD] https://orcid.org/0000-0002-1028-8445

Adetola B Adesida [iD] https://orcid.org/0000-0003-1798-6251

Supplemental material

Supplemental material for this article is available online.

References

1. Makris EA, Hadidi P and Athanasiou KA. The knee meniscus: structure-function, pathophysiology, current repair techniques, and prospects for regeneration. *Biomaterials* 2011; 32: 7411–7431.
2. Andrews SHJ, Adesida AB, Abusara Z, et al. Current concepts on structure–function relationships in the menisci. *Connect Tissue Res* 2017; 58: 271–281.
3. Arnoczky SP and Warren RF. Microvasculature of the human meniscus. *Am J Sports Med* 1982; 10: 90–95.
4. Lohmander LS, Englund PM, Dahl LL, et al. The long-term consequence of anterior cruciate ligament and meniscus injuries. *Am J Sports Med* 2007; 35: 1756–1769.
5. Rangger C, Klestil T, Gloetzer W, et al. Osteoarthritis after arthroscopic partial meniscectomy. *Am J Sports Med* 1995; 23: 240–244.
6. Clark CR and Ogden JA. Development of the menisci of the human knee joint. Morphological changes and their potential role in childhood meniscal injury. *J Bone Joint Surg Am* 1983; 65: 538–547.
7. Fox AJS, Bedi A and Rodeo SA. The basic science of human knee menisci. *Sports Health* 2012; 4: 340–351.
8. Sanchez-Adams J and Athanasiou KA. The knee meniscus: a complex tissue of diverse cells. *Cell Mol Bioeng* 2009; 2: 332–340.
9. Lund-Olesen K. Oxygen tension in synovial fluids. *Arthritis Rheum* 1970; 13: 769–776.
10. Adesida AB, Grady LM, Khan WS, et al. The matrix-forming phenotype of cultured human meniscus cells is enhanced after culture with fibroblast growth factor 2 and is further stimulated by hypoxia. *Arthritis Res Ther* 2006; 8: R61.
11. Szojka ARA, Lyons BD, Moore CN, et al. Hypoxia and TGF-β3 synergistically mediate inner meniscus-like matrix formation by fibrochondrocytes. *Tissue Eng Part A* 2018; 25: 446–456.
12. Tan GK, Dinnes DLM, Myers PT, et al. Effects of biomimetic surfaces and oxygen tension on redifferentiation of passaged human fibrochondrocytes in 2D and 3D cultures. *Biomaterials* 2011; 32: 5600–5614.
13. Gunja NJ and Athanasiou KA. Additive and synergistic effects of bFGF and hypoxia on leporine meniscus cell-seeded PLLA scaffolds. *J Tissue Eng Regen Med* 2010; 4: 115–122.
14. Gunja NJ and Athanasiou KA. Effects of hydrostatic pressure on leporine meniscus cell-seeded PLLA scaffolds. *J Biomed Mater Res Part A* 2009; 92A: 896–905.
15. Ballyns JJ and Bonassar LJ. Dynamic compressive loading of image-guided tissue engineered meniscal constructs. *J Biomech* 2011; 44: 509–516.
16. Mauck RL, Soltz MA, Wang CCB, et al. Functional tissue engineering of articular cartilage through dynamic loading of chondrocyte-seeded agarose gels. *J Biomech Eng* 2000; 122: 252–260.
17. Liang Y, Idrees E, Andrews SHJ, et al. Plasticity of human meniscus fibrochondrocytes: a study on effects of mitotic divisions and oxygen tension. *Sci Rep* 2017; 7: 12148.
18. Scholtes S, Krämer E, Weisser M, et al. Global chondrocyte gene expression after a single anabolic loading period: time evolution and re-inducibility of mechano-responses. *J Cell Physiol* 2018; 233: 699–711.
19. Fitzgerald JB, Jin M, Dean D, et al. Mechanical compression of cartilage explants induces multiple time-dependent gene expression patterns and involves intracellular calcium and cyclic AMP. *J Biol Chem* 2004; 279: 19502–19511.
20. Baker BM, Nathan AS, Huffman GR, et al. Tissue engineering with meniscus cells derived from surgical debris. *Osteoarthritis Cartilage* 2009; 17: 336–345.
21. Anderson DE and Johnstone B. Dynamic mechanical compression of chondrocytes for tissue engineering: a critical review. *Front Bioeng Biotechnol* 2017; 5: 76.
22. Pauli C, Grogan SP, Patil S, et al. Macroscopic and histopathologic analysis of human knee menisci in aging and osteoarthritis. *Osteoarthritis Cartilage* 2011; 19: 1132–1141.
23. Gamer LW, Shi RR, Gendelman A, et al. Identification and characterization of adult mouse meniscus stem/progenitor cells. *Connect Tissue Res* 2017; 58: 238–245.
24. Sun H, Wen X, Li H, et al. Single-cell RNA-seq analysis identifies meniscus progenitors and reveals the progression of meniscus degeneration. *Ann Rheum Dis* 2019; 79: 408–417.
25. Shen W, Chen J, Zhu T, et al. Intra-articular injection of human meniscus stem/progenitor cells promotes meniscus regeneration and ameliorates osteoarthritis through stromal cell-derived factor-1/CXCR4-mediated homing. *Stem Cells Transl Med* 2014; 3: 387–394.
26. Muhammad H, Schminke B, Bode C, et al. Human migratory meniscus progenitor cells are controlled via the TGF-β pathway. *Stem Cell Reports* 2014; 3: 789–803.

27. Muhammad H. *Human and mouse meniscus progenitor cells and their role in meniscus tissue regeneration*. PhD Thesis, Georg-August University, 2014.

28. Buma P, Ramrattan NN, Van Tienen TG, et al. Tissue engineering of the meniscus. *Biomaterials* 2004; 25: 1523–1532.

29. Adesida A, Millward-Sadler S and Hardingham T. Human meniscus cells contain a progenitor cell population. In: *The Centenary (190th) Meeting of the Pathological Society of Great Britain and Ireland*. The Journal of Pathology, https://onlinelibrary.wiley.com/doi/10.1002/path.2052 (2006, accessed 25 September 2020).

30. Matsukura Y, Muneta T, Tsuji K, et al. Mesenchymal stem cells in synovial fluid increase after meniscus injury. *Clin Orthop Relat Res* 2014; 472: 1357–1364.

31. Tarafder S, Gulko J, Sim KH, et al. Engineered healing of avascular meniscus tears by stem cell recruitment. *Sci Rep* 2018; 8: 8150.

32. Elkhenany H, Szojka >ARA, Mulet-Sierra A, et al. Bone marrow mesenchymal stem cells-derived tissues are mechanically superior to meniscus cells'. *Tissue Eng Part A*. Epub ahead of print October 2020. DOI: 10.1089/ten.TEA.2020.0183.

33. Grogan SP, Duffy SF, Pauli C, et al. Gene expression profiles of the meniscus avascular phenotype: a guide for meniscus tissue engineering. *J Orthop Res* 2018; 36: 1947–1958.

34. Meyer EG, Buckley CT, Thorpe SD, et al. Low oxygen tension is a more potent promoter of chondrogenic differentiation than dynamic compression. *J Biomech* 2010; 43: 2516–2523.

35. Wernike E, Li Z, Alini M, et al. Effect of reduced oxygen tension and long-term mechanical stimulation on chondrocyte-polymer constructs. *Cell Tissue Res* 2008; 331: 473–483.

36. Hansen U, Schunke M, Domm C, et al. Combination of reduced oxygen tension and intermittent hydrostatic pressure: a useful tool in articular cartilage tissue engineering. *J Biomech* 2001; 34: 941–949.

37. Okada K, Mori D, Makii Y, et al. Hypoxia-inducible factor-1 alpha maintains mouse articular cartilage through suppression of NF-κB signaling. *Sci Rep* 2020; 10: 1–11.

38. Adesida AB, Grady LM, Khan WS, et al. Human meniscus cells express hypoxia inducible factor-1α and increased SOX9 in response to low oxygen tension in cell aggregate culture. *Arthritis Res Ther* 2007; 9: R69.

39. Adesida AB, Mulet-Sierra A, Laouar L, et al. Oxygen tension is a determinant of the matrix-forming phenotype of cultured human meniscal fibrochondrocytes. *PLoS One* 2012; 7: e39339.

40. AufderHeide AC and Athanasiou KA. Mechanical stimulation toward tissue engineering of the knee meniscus. *Ann Biomed Eng* 2004; 32: 1163–1176.

41. Upton ML, Chen J, Guilak F, et al. Differential effects of static and dynamic compression on meniscal cell gene expression. *J Orthop Res* 2003; 21: 963–969.

42. Imler SM, Doshi AN and Levenston ME. Combined effects of growth factors and static mechanical compression on meniscus explant biosynthesis. *Osteoarthritis Cartilage* 2004; 12: 736–744.

43. Huey DJ and Athanasiou KA. Tension-compression loading with chemical stimulation results in additive increases to functional properties of anatomic meniscal constructs. *PLoS One* 2011; 6(11): e27857.

44. Puetzer JL, Brown BN, Ballyns JJ, et al. The effect of IGF-I on anatomically shaped tissue-engineered menisci. *Tissue Eng Part A* 2013; 19: 1443–1450.

45. Puetzer JL and Bonassar LJ. Physiologically distributed loading patterns drive the formation of zonally organized collagen structures in tissue-engineered meniscus. *Tissue Eng Part A* 2016; 22: 907–916.

46. McNulty AL and Guilak F. Mechanobiology of the meniscus. *J Biomech* 2015; 48: 1469–1478.

47. Griffin TM and Guilak F. The role of mechanical loading in the onset and progression of osteoarthritis. *Exerc Sport Sci Rev* 2005; 33: 195–200.

48. Lima EGG, Bian L, Ng KWW, et al. The beneficial effect of delayed compressive loading on tissue-engineered cartilage constructs cultured with TGF-β3. *Osteoarthritis Cartilage* 2007; 15: 1025–1033.

49. Suzuki T, Toyoda T, Suzuki H, et al. Hydrostatic pressure modulates mRNA expressions for matrix proteins in human meniscal cells. *Biorheology* 2006; 43: 611–622.

50. Zellner J, Mueller M, Xin Y, et al. Dynamic hydrostatic pressure enhances differentially the chondrogenesis of meniscal cells from the inner and outer zone. *J Biomech* 2015; 48: 1479–1484.

51. Baker B, Shah R, Silverstein A, et al. Dynamic tension improves the mechanical properties of nanofiber-based engineered meniscus constructs. In: *Transactions of the 56th annual meeting of the Orthopaedic Research Society*, Vol. 35, paper 0179 (accessed 30 March 2020).

52. Furumatsu T, Kanazawa T, Yokoyama Y, et al. Inner meniscus cells maintain higher chondrogenic phenotype compared with outer meniscus cells. *Connect Tissue Res* 2011; 52: 459–465.

53. Furumatsu T, Kanazawa T, Miyake Y, et al. Mechanical stretch increases Smad3-dependent CCN2 expression in inner meniscus cells. *J Orthop Res* 2012; 30: 1738–1745.

54. Petersen W and Tillmann B. Age-related blood and lymph supply of the knee menisci:a cadaver study. *Acta Orthop* 1995; 66: 308–312.

55. Pufe T, Petersen WJ, Miosge N, et al. Endostatin/collagen XVIII - an inhibitor of angiogenesis - is expressed in cartilage and fibrocartilage. *Matrix Biol* 2004; 23: 267–276.

56. Fukazawa I, Hatta T, Uchio Y, et al. Development of the meniscus of the knee joint in human fetuses. *Congenit Anom (Kyoto)* 2009; 49: 27–32.

57. McMurray TP. The semilunar cartilages. *Br J Surg* 1942; 29: 407–414.

58. Clark C and Ogden J. Prenatal and postnatal development of human knee joint menisci. *Iowa Orthop J* 1981; 1: 20–27.

59. Thoms BL, Dudek KA, Lafont JE, et al. Hypoxia promotes the production and inhibits the destruction of human articular cartilage. *Arthritis Rheum* 2013; 65: 1302–1312.

60. Stone AV, Loeser RF, Callahan MF, et al. Role of the hypoxia-inducible factor pathway in normal and osteoarthritic meniscus and in mice after destabilization of the medial meniscus. *Cartilage*. Epub ahead of print 17 September 2020. DOI: 10.1177/1947603520958143.